

Perturbation Theory of Scattering Amplitudes at High Energies

JAMES D. BJORKEN* AND TAI TSUN WU†
Institute for Advanced Study, Princeton, New Jersey
 (Received 13 February 1963)

The asymptotic behavior of Feynman-Dyson graphs for elastic scattering at high energies is studied by means of the Mellin transform. The leading terms of a set of graphs involving three-particle intermediate states are summed. Under certain conditions the asymptotic behavior of the sum is found to contain a factor $(\ln s)^{-3/2}$. This is incompatible with Regge behavior, but is consistent instead with a cut in the complex angular momentum plane.

1. INTRODUCTION

IN view of Regge's detailed analysis¹ of potential scattering for large (and unphysical) momentum transfers, it has been conjectured that similar behaviors also hold for elastic scattering in field theory. By crossing symmetry, this conjecture leads to definite predictions for elastic differential cross sections at high energies. To gain a better understanding of these predictions, several authors²⁻⁵ have studied the elastic scattering amplitude at high energies by perturbation theory. In each case the result is found to be consistent with Regge behavior.

In the cases considered by these authors,²⁻⁵ two-particle intermediate states seem to play a predominant role. Thus, these cases are perhaps in closer analog to potential scattering than the more general situations in field theory. It is the purpose of this paper to study a different special case where two- and three-particle intermediate states play comparable roles. Because of the inclusion of three-particle states, the computation becomes more complicated. To reduce this complication, a more streamlined procedure is proposed where the Mellin transform is essential. After a short discussion of the Mellin transform in Sec. 2, the proposed procedure is applied to the simple case of the ladder graphs in Sec. 3. The special case of interest is worked through in Sec. 4, and discussed in Sec. 5. The result is that Regge behavior is not obtained in the present case; instead, it is consistent with a branch cut in the angular momentum plane.

2. MELLIN TRANSFORM

The Mellin transform consists of the pair of integrals

$$F(\alpha) = \int_0^\infty f(s) s^{-\alpha-1} ds, \quad (1a)$$

and

$$f(s) = \frac{1}{2\pi i} \int_C F(\alpha) s^\alpha d\alpha, \quad (1b)$$

where the contour C is a straight line from $c-i\infty$ to $c+i\infty$, provided that $F(\alpha)$ is analytic on this line. Equations (1) are merely the Fourier integral formula in the variables $\ln s$ and $-i\alpha$. In particular, when

$$f(s) = \begin{cases} s^{-a} (\ln s)^b & \text{for } s > 1, \\ 0 & \text{for } s \leq 1, \end{cases} \quad (2)$$

$F(\alpha)$ is given by

$$F(\alpha) = \Gamma(b+1) (\alpha+a)^{-b-1}. \quad (3)$$

Here c can be taken to be any number larger than $-a$, and, when b is not an integer, the branch cut in (3) may be taken to be the straight line from $-\infty$ to $-a$.

3. LADDER GRAPHS

Throughout the present consideration, spins are ignored and the Lagrangian density is taken to be

$$L = L_0 + L_1, \quad (4)$$

where

$$L_0 = -\frac{1}{2} \sum_{\mu=1}^4 (\partial\phi/\partial x_\mu)^2 - \frac{1}{2} \phi^2, \quad (5)$$

and

$$L_1 = \frac{1}{3} (2\pi)^3 g \phi^3 + \frac{1}{6} (2\pi)^2 G \phi^4. \quad (6)$$

Here units have been so chosen that $\hbar=c=m=1$. For this Lagrangian density, the Feynman-Dyson rules are as follows: $-i(k^2+m^2-i\epsilon)^{-1}$ for a propagator, ig/π for a three-point vertex, and iG/π^2 for a four-point vertex.

In this section, let $G=0$ and consider the ladder graphs as shown in Fig. 1. The contribution from such a

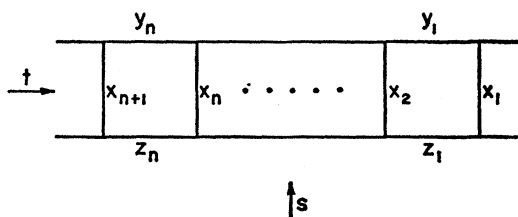


FIG. 1. The ladder graph.

* Alfred P. Sloan Foundation Fellow.
 † Alfred P. Sloan Foundation Fellow. On leave from Harvard University, Cambridge, Massachusetts.
¹ T. Regge, *Nuovo Cimento* 14, 951 (1959).
² M. Gell-Mann and M. L. Goldberger, *Phys. Rev. Letters* 9, 275 (1962).
³ M. Lévy (to be published).
⁴ J. C. Polkinghorne (to be published).
⁵ P. G. Federbush and M. T. Grisaru (to be published).

graph, expressed in terms of Feynman parameters, is given by

$$\mathcal{L}_n = K (ig^2)^{n+1} \int_0^\infty \cdots \int_0^\infty dx_1 \cdots dx_{n+1} dy_1 \cdots dy_n \times dz_1 \cdots dz_n \Delta^{-2} e^{iQ}, \quad (7)$$

where Δ is the network determinant, Q is a linear function of s and t , and K is a constant independent of n . It is desired to obtain the behavior of \mathcal{L}_n for large s but fixed t . The function Q has the form

$$Q = s\Delta^{-1} \prod_{i=1}^{n+1} x_i + J, \quad (8)$$

where J is independent of s . Let $L_n(\alpha)$ be the Mellin transform of \mathcal{L}_n as defined by (1), then

$$L_n(\alpha) = K (ig^2)^{n+1} e^{-i\frac{1}{2}\alpha\pi} \Gamma(-\alpha) \int_0^\infty \cdots \int_0^\infty dx_1 \cdots dx_{n+1} \times dy_1 \cdots dy_n dz_1 \cdots dz_n \Delta^{-2-\alpha} \left(\prod_{i=1}^{n+1} x_i^\alpha \right) e^{iJ}. \quad (9)$$

The asymptotic behavior of \mathcal{L}_n is determined by the behavior of $L_n(\alpha)$ near $\alpha = -1$. By (9), it is sufficient to consider the region where x_i are all small. Hence, $L_n(\alpha)$ may be approximated by

$$L_n(\alpha) \sim K (ig^2)^{n+1} e^{-i\frac{1}{2}\alpha\pi} \Gamma(-\alpha) \int_0^\infty \cdots \int_0^\infty dy_1 \cdots dy_n \times dz_1 \cdots dz_n \int_0^\tau \cdots \int_0^\tau dx_1 \cdots dx_{n+1} \times \Delta_0^{-2-\alpha} \left(\prod_{i=1}^{n+1} x_i^\alpha \right) e^{iJ_0}, \quad (10)$$

where τ is a small but fixed quantity, Δ_0 and J_0 are the values of Δ and J , respectively, for all $x_i = 0$. More explicitly,

$$\Delta_0 = \prod_{i=1}^n (y_i + z_i), \quad (11a)$$

and

$$J_0 = \sum_{i=1}^n \left[t \left(\frac{y_i z_i}{y_i + z_i} \right) - (1 - i\epsilon)(y_i + z_i) \right]. \quad (11b)$$

Equation (10) leads immediately to

$$L_n(\alpha) \sim K (ig^2)^{n+1} e^{-i\frac{1}{2}\alpha\pi} \Gamma(-\alpha) [(\alpha+1)^{-1} \tau^{\alpha+1}]^{n+1} \times [-i\gamma_\alpha(t)]^n, \quad (12)$$

where

$$\gamma_\alpha(t) = i \int_0^\infty \int_0^\infty dy dz (y+z)^{-2-\alpha} \times \exp \left\{ i \left[t \frac{yz}{y+z} - (1-i\epsilon)(y+z) \right] \right\}. \quad (13)$$

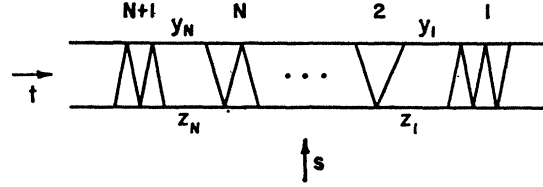


FIG. 2. A truss-bridge graph.

Since (12) is valid only near $\alpha = -1$, it may be simplified to

$$L_n(\alpha) \sim -K g^{2(n+1)} (\alpha+1)^{-n-1} [\gamma_{-1}(t)]^n. \quad (14)$$

By (13), $\gamma_{-1}(t)$ is given by

$$\gamma_{-1}(t) = \int_0^1 dy [1 - ty(1-y)]^{-1} = \left[-\frac{1}{4}t(1-\frac{1}{4}t) \right]^{-1/2} \tanh^{-1}(1-4t)^{-1/2}. \quad (15)$$

Comparison of (14) with (2) and (3) then yields the desired result that for large s

$$\mathcal{L}_n(s) \sim -K g^{2(n+1)} [\gamma_{-1}(t)]^n s^{-1} (\ln s)^n / n!. \quad (16)$$

This is the result obtained by Polkinghorne,⁴ Federbush and Grisaru.⁵ When summed over n , (16) is found to be consistent with the idea of Regge poles. In particular, it agrees with the earlier result obtained by Lee and Sawyer⁶ using Fredholm theory.

4. TRUSS-BRIDGE GRAPHS

The purpose of this paper is to apply the method of the Mellin transform to the "truss-bridge" graphs, as shown in Fig. 2.

A.

Consider first the special case where there is no two-particle intermediate state, as shown in Fig. 3. Similar to (7), the contribution from this graph is given by

$$\mathfrak{M}_n = iK g^2 G^n \int_0^\infty \cdots \int_0^\infty dx_1 \cdots dx_{n+1} \times du_1 \cdots du_n \Delta(n)^{-2} e^{iQ}, \quad (17)$$

where Δ and Q are those functions pertaining to the present graph, and are, of course, in no way related to

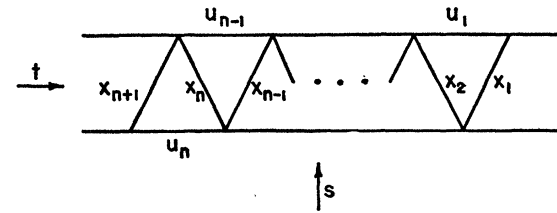


FIG. 3. The truss-bridge graph without two-particle intermediate states.

⁶ B. W. Lee and R. F. Sawyer, Phys. Rev. **127**, 2266 (1962).

those of (7). However, the s dependence of Q may again be given explicitly by (8). Let $M_n(\alpha)$ be the Mellin transform of \mathfrak{M}_n . Then

$$M_n(\alpha) = iKg^2G^n e^{-i\frac{1}{2}\pi\alpha} \Gamma(-\alpha) \int_0^\infty \cdots \int_0^\infty dx_1 \cdots dx_{n+1} \times du_1 \cdots du_n \Delta(n)^{-2-\alpha} \left(\prod_{i=1}^{n+1} x_i^\alpha \right) e^{iJ}. \quad (18)$$

This is in close analog with (9). Again, the behavior of \mathfrak{M}_n for large s but fixed t may be found by studying $M_n(\alpha)$ for α near -1 .

In view of the close analog, it is tempting to follow

$$M_n(\alpha) \sim -Kg^2G^n \int_0^\tau \cdots \int_0^\tau dx_1 \cdots dx_{n+1} du_1 \cdots du_n \Delta(n)^{-2-\alpha} \prod_{i=1}^{n+1} x_i^\alpha = -Kg^2G^n \tau^{1+\alpha} \int_0^1 \cdots \int_0^1 dx_1 \cdots dx_{n+1} du_1 \cdots du_n \Delta(n)^{-2-\alpha} \prod_{i=1}^{n+1} x_i^\alpha \sim -Kg^2G^n \int_0^1 \cdots \int_0^1 dx_1 \cdots dx_{n+1} du_1 \cdots du_n \Delta(n)^{-2-\alpha} \prod_{i=1}^{n+1} x_i^\alpha. \quad (20)$$

This integral may be evaluated by using recurrence formulas. If $\Delta'(n)$ is the network determinant for the graph shown in Fig. 4, then

$$\Delta(n) = x_{n+1}\Delta(n-1) + \Delta'(n), \quad (21a)$$

and

$$\Delta'(n) = u_n\Delta(n-1) + x_n\Delta'(n-1). \quad (21b)$$

In particular,

$$\Delta(0) = \Delta'(0) = 1, \quad (22)$$

$$\Delta(1) = x_1 + x_2 + u_1, \quad (23a)$$

and

$$\Delta'(1) = x_1 + u_1. \quad (23b)$$

In order to get the recurrence formula, define, for p any non-negative integer,

$$A(\alpha, n, p) = \int_0^1 \cdots \int_0^1 dx_1 \cdots dx_{n+1} du_1 \cdots du_n \times \Delta(n)^{-2-\alpha} x_1^\alpha \cdots x_{n+1}^\alpha \left[\ln \frac{\Delta(n)}{x_{n+1}\Delta'(n)} \right]^p. \quad (24)$$

Then it follows from (20) that near $\alpha = -1$

$$M_n(\alpha) \sim -Kg^2G^n A(\alpha, n, 0). \quad (25)$$

It is shown in Appendix I by using (21) that near $\alpha = -1$

$$A(\alpha, n, p) \sim p!(1+\alpha)^{-2n-p-1} B(n, p), \quad (26)$$

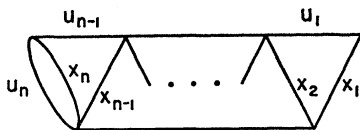


FIG. 4. The graph that defines $\Delta'(n)$.

the procedure of the last section. However, this does not lead to any meaningful result. More precisely, in the present case, what corresponds to $\gamma_\alpha(t)$ is

$$i \int_0^\infty du u^{-2-\alpha} \exp[-i(1-i\epsilon)u],$$

or simply

$$-e^{\frac{1}{2}\pi\alpha} \Gamma(-1-\alpha). \quad (19)$$

This expression (19) is not bounded near $\alpha = -1$. This means that the contribution to $M_n(\alpha)$ for α near -1 comes mainly from the region where all x_i and all u_i are small. Hence, Δ cannot be approximated by Δ_0 but J may be replaced by 0. This consideration leads to

and moreover $B(n, p)$ satisfies

$$B(n, p) = \sum_{m=1}^{p+1} B(n-1, m) \quad \text{for } p \geq 0, \quad (27)$$

together with

$$B(0, p) = 1 \quad \text{for } p \geq 0. \quad (28)$$

The difference equation (27) with (28) as the boundary condition is solved in Appendix II.

A comparison of (25) with (3) gives that for large s

$$\mathfrak{M}_n \sim -Kg^2G^n B(n, 0) s^{-1} (\ln s)^{2n} / n!. \quad (29)$$

As in the case of the ladder graphs, it is now assumed that the asymptotic behavior of the sum for large s

$$\mathfrak{M} = \sum_{n=0}^\infty \mathfrak{M}_n (2 - \delta_{n0}) \quad (30)$$

is given by the sum of the leading terms. Under this assumption, the Mellin transform of \mathfrak{M} is given by

$$M(\alpha) \sim -Kg^2(1+\alpha)^{-1} \sum_{n=0}^\infty (2 - \delta_{n0}) B(n, 0) [G(1+\alpha)^{-2}]^n = -Kg^2(1+\alpha)^{-1} \{ 2f[G(1+\alpha)^{-2}] - 1 \} = -Kg^2G^{-1} \{ 1 + \alpha - [(1+\alpha)^2 - 4G]^{-1} - G(1+\alpha)^{-1} \}, \quad (31)$$

where f is given by (B7). Thus, $M(\alpha)$ has branch points at

$$\alpha = -1 \pm 2G^{1/2}. \quad (32a)$$

When $G < 0$, the dominating terms for \mathfrak{M}_n alternate in

sign, and thus the present result must be considered to be more unreliable. Thus, it is assumed hereafter that $G \geq 0$. From (31), the inverse Mellin transform \mathfrak{M} can be explicitly computed to be

$$\mathfrak{M} \sim -K g^2 s^{-1} [-1 + 2(G^{1/2} \ln s)^{-1} I_1(2G^{1/2} \ln s)], \quad (32b)$$

where I is the modified Bessel function. If $G=0$, then

$$\mathfrak{M} \sim -K g^2 s^{-1} \quad (33a)$$

as expected. If $G > 0$, then for s sufficiently large

$$\mathfrak{M} \sim -K g^2 \pi^{1/2} s^{-1+2\sqrt{G}} (G^{1/2} \ln s)^{-3/2}. \quad (33b)$$

B.

Attention is now turned to the more general case of the truss-bridge graph with possibly two-particle intermediate states. Since in the case of $M_n(\alpha)$, only the region where all x and all u are small is significant, here it is possible to follow the procedure of Sec. 3. With reference to Fig. 2, consider a case where there are N two-particle states in the t channel, and hence there are $N+1$ "sections." Let $\Delta_1, \Delta_2, \dots, \Delta_{N+1}$ be the network determinants, and n_1, n_2, \dots, n_{N+1} the numbers of G 's of the $N+1$ sections. Then, the contribution from this graph is given approximately by

$$\begin{aligned} & \mathfrak{M}(n_1, n_2, \dots, n_{N+1}) \\ & \sim K (i g^2)^{N+1} G^{n_1+n_2+\dots+n_{N+1}} \int_0^\infty \dots \int_0^\infty dy_1 \dots dy_N \\ & \quad \times dz_1 \dots dz_N \int_0^\tau \dots \int_0^\tau d\alpha_1 \dots d\alpha_{N+1} \\ & \quad \times \Delta_0^{-2} \exp[i s (\prod_{i=1}^{N+1} \zeta_i) / \Delta_0] \exp(i \mathbf{J}_0), \quad (34) \end{aligned}$$

where

$$\Delta_0 = \left[\prod_{i=1}^N (y_i + z_i) \right] \prod_{i=1}^{N+1} \Delta_i, \quad (35)$$

$$\mathbf{J}_0 = \sum_{i=1}^N \left[i \left(\frac{y_i z_i}{y_i + z_i} \right) - (1 - i\epsilon)(y_i + z_i) \right], \quad (36)$$

and $d\alpha_i$ and ζ_i are, respectively, $(\prod dx)$ $(\prod du)$ and $\prod x$ for section i . For α near -1 , the Mellin transform of (34) gives

$$\begin{aligned} & \mathbf{M}(\alpha; n_1, n_2, \dots, n_{N+1}) \\ & \sim i K (i g^2)^{N+1} G^{n_1+\dots+n_{N+1}} \int_0^\infty \dots \int_0^\infty dy_1 \dots dy_N \\ & \quad \times dz_1 \dots dz_N \int_0^\tau \dots \int_0^\tau d\alpha_1 \dots d\alpha_{N+1} \\ & \quad \times \Delta_0^{-2-\alpha} \zeta_1^\alpha \dots \zeta_{N+1}^\alpha \exp(i \mathbf{J}_0) \\ & \sim -K \prod_{i=1}^{N+1} [-M(n_i)/K] [\gamma_{-1}(t)]^N, \quad (37) \end{aligned}$$

where $\gamma_{-1}(t)$ is given by (15). Let \mathfrak{M} be the sum of $\mathfrak{M}(n_1, \dots, n_{N+1})$ over all possible truss-bridge graphs, then by (31)

$$\mathbf{M}(\alpha) \sim M(\alpha) [1 + K^{-1} M(\alpha) \gamma_{-1}(t)]^{-1}. \quad (38)$$

This is the desired result.

It only remains to obtain some simple properties of the right-hand side of (38). Since the right-hand side of (31), with the factor $-K$ removed, is monotonically decreasing for $\alpha > -1 + 2G^{1/2}$, and by (31)

$$M(-1 + 2G^{1/2}) \sim -\frac{2}{3} K g^2 G^{-1/2}, \quad (39)$$

the quantity in the brackets of (38) has a zero

$$\alpha_0(t) > -1 + 2G^{1/2}, \quad (40)$$

if and only if

$$\gamma_{-1}(t) > \frac{2}{3} g^{-2} G^{1/2}. \quad (41)$$

Note that (41) is always satisfied if $G=0$. If $G > 0$, (41) can be satisfied only for sufficiently small momentum transfer. If (41) is satisfied, then for large s

$$\mathfrak{M} \sim \text{const } s^{\alpha_0(t)}. \quad (42)$$

On the other hand, if

$$\gamma_{-1}(t) < \frac{2}{3} g^{-2} G^{1/2}, \quad (43)$$

then for large s

$$\mathfrak{M} \sim -K g^2 \pi^{1/2} [1 - \frac{2}{3} g^2 G^{-1/2} \gamma_{-1}(t)] \times s^{-1+2\sqrt{G}} (G^{1/2} \ln s)^{-3/2}, \quad (44)$$

by (33b). The transition between (42) and (44) is complicated.

5. CHOICE OF GRAPHS

The choice of the truss-bridge graphs still need to be discussed. Only the motivation can be described, and such a discussion is at best heuristic. In the considerations of Polkinghorne,⁴ Federbush and Grisaru,⁵ in each case a small number of graphs for elastic scattering is first selected, and then these graphs are iterated in the t channel to give all the graphs taken into account. Hence, in their work, two-particle intermediate states play an exceptionally important role. It is the purpose here to treat the three-particle intermediate states in an analogous way. More precisely, the procedure followed consists of the following steps: (1) Choose the six elementary graphs shown in Fig. 5; (2) combine all permissible sequences of these elementary graphs in the t channel to get graphs for elastic scattering; (3) for each order of the coupling constants g and G , compute the leading term for large s ; and (4) add up these leading terms.

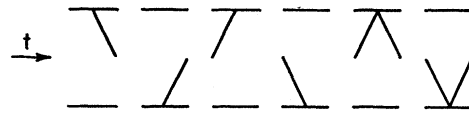


FIG. 5. The six elementary graphs.

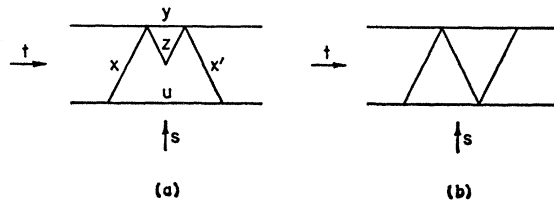


FIG. 6. Two graphs of the same order.

The question is immediately raised that, in step (2), graphs other than the truss-bridge graphs are obtained. A simple example is shown in Fig. 6(a). This graph is divergent, but renormalization is simple. In Appendix III, it is shown that the contribution from this graph is very small when $s \rightarrow \infty$ as compared with that from the graph of Fig. 6(b), a graph of the same order in the coupling constants. Thus, by step (3), the graph of Fig. 6(a) may be omitted. Although a rigorous proof is still lacking, in general, for the purpose of step (3) only truss-bridge graphs need to be considered.

6. DISCUSSIONS

Numerous questions may be raised with respect to the procedure outlined in the last section. Although the idea of summing the dominating terms of a series has been used successfully in a number of physical problems, the validity has only been established in cases where an independent calculation is available.⁶ The choice of graphs is a difficulty peculiar to the present problem, and the relevance of the particular choice can by no means be taken for granted. However, if the procedure is assumed to be valid, then under the condition (43) the asymptotic behavior of the scattering amplitude at high energies contains a negative fractional power of the logarithm of the energy, as given by (44).

Although the Mellin transform plays an essential role in the present consideration, it is introduced for mathematical convenience rather than on physical grounds. Indeed, the complex α -plane does not seem to have any direct physical interpretation. However, when a branch cut is found in the complex α plane for the case studied, this implies a certain asymptotic behavior for the elastic scattering amplitude at high energies, and this in turn necessitates the presence of at least a branch cut in the complex angular momentum plane.

Branch cuts in the angular momentum plane have also been found in the case of potential scattering for particles with nonzero spin. However, these branch cuts are kinematical in nature. Moreover, they do not lead to logarithmic dependence on the energy for differential elastic scattering cross sections.⁷ Hence,

⁷ J. M. Charap and E. J. Squires, *Ann. Phys. (N. Y.)* (to be published). We would like to thank Dr. J. M. Charap and Professor R. Oehme for helpful discussion on this point.

these branch cuts may be thought of as a peculiarity of the definition of the S matrix. Oehme⁸ has also found branch cuts for a Klein-Gordon particle in a static Coulomb potential; however, his cuts are related to the existence of a r^{-2} potential and is consequently of a dynamic origin. The branch cut for the present case comes from detailed properties of Feynman-Dyson graphs, and is, therefore, also directly related to the dynamics of the system under consideration.

It is the original purpose of this work to study the effect of three-particle intermediate states on high-energy behaviors. The detailed connection between the three-particle intermediate states and the appearance of a cut is not understood by the authors. If these three-particle states are indeed responsible for the appearance of the branch cut in the angular momentum plane, then it is perhaps reasonable to conjecture that the scattering amplitude, as a function of the complex angular momentum, has many branch points, even apart from the kinematic ones, in the case of relativistic field theory where the number of particles is not a constant of the motion.

ACKNOWLEDGMENTS

For very helpful discussions, we are greatly indebted to Professor C. N. Yang and Professor P. G. Federbush. We would also like to thank Professor J. R. Oppenheimer for his hospitality at the Institute for Advanced Study.

APPENDIX I

In this Appendix, (26) and (27) are to be derived. If ϕ and ψ are two positive constants, then it is easily verified that

$$\int_0^\infty \frac{dx x^\alpha}{(\phi x + \psi)^{2+\alpha}} \left[\ln \frac{\phi x + \psi}{\psi x} \right]^p = \psi^{-1} \phi^{-1-\alpha} p! \sum_{k=0}^p (1+\alpha)^{-p+k-1} [\ln(\phi/\psi)]^k / k!, \quad (\text{A1})$$

and

$$\int_0^1 \frac{du}{\phi u + \psi} \left[\ln \frac{\phi}{\phi u + \psi} \right]^p = (p+1)^{-1} \phi^{-1} \left[\left(\ln \frac{\phi}{\psi} \right)^{p+1} - \left(\ln \frac{\phi}{\phi + \psi} \right)^{p+1} \right]. \quad (\text{A2})$$

With these equalities (21) may be substituted into

⁸ R. Oehme, *Nuovo Cimento* **25**, 183 (1962).

(24) to yield

$$\begin{aligned}
 A(\alpha, n, p) &= \int_0^1 \cdots \int_0^1 dx_1 \cdots dx_n du_1 \cdots du_n x_1^\alpha \cdots x_n^\alpha \int_0^1 \frac{dx_{n+1} x_{n+1}^\alpha}{[x_{n+1} \Delta(n-1) + \Delta'(n)]^{2+\alpha}} \left\{ \ln \frac{x_{n+1} \Delta(n-1) + \Delta'(n)}{x_{n+1} \Delta'(n)} \right\}^p \\
 &\sim \int_0^1 \cdots \int_0^1 dx_1 \cdots dx_n du_1 \cdots du_n x_1^\alpha \cdots x_n^\alpha p! \Delta'(n)^{-1} \Delta(n-1)^{-1-\alpha} \sum_{k=0}^p (1+\alpha)^{-p+k-1} \{ \ln [\Delta(n-1)/\Delta'(n)] \}^k / k! \\
 &= \int_0^1 \cdots \int_0^1 dx_1 \cdots dx_n du_1 \cdots du_{n-1} x_1^\alpha \cdots x_n^\alpha p! \Delta(n-1)^{-1-\alpha} \\
 &\quad \times \sum_{k=0}^p (1+\alpha)^{-p+k-1} \frac{1}{k!} \int_0^1 \frac{du_n}{u_n \Delta(n-1) + x_n \Delta'(n-1)} \left[\ln \frac{\Delta(n-1)}{u_n \Delta(n-1) + x_n \Delta'(n-1)} \right]^k \\
 &= \int_0^1 \cdots \int_0^1 dx_1 \cdots dx_n du_1 \cdots du_{n-1} x_1^\alpha \cdots x_n^\alpha p! \Delta(n-1)^{-2-\alpha} \sum_{k=0}^p (1+\alpha)^{-p+k-1} \frac{1}{(k+1)!} \\
 &\quad \times \left\{ \left[\ln \frac{\Delta(n-1)}{x_n \Delta'(n-1)} \right]^{k+1} - \left[\ln \frac{\Delta(n-1)}{\Delta(n-1) + x_n \Delta'(n-1)} \right]^{k+1} \right\} \\
 &\sim p! \sum_{m=1}^{p+1} (1+\alpha)^{-p+m-2} A(\alpha, n-1, m) / m!. \tag{A3}
 \end{aligned}$$

On the other hand, it follows from setting $n=0$ that

$$A(\alpha, 0, p) = \int_0^1 dx x^\alpha (-\ln x)^p = (1+\alpha)^{-p-1} p!. \tag{A4}$$

Equation (26) follows from (A3) and (A4); (28) from (A4) and (26); and the substitution of (26) into (A3) gives (27).

APPENDIX II

In this Appendix, the difference equation (27) is to be solved with the boundary condition (28). First, it follows from (27) and (28) that

$$0 < B(n, p) \leq 2^{2n+p}. \tag{B1}$$

Therefore, the function

$$b(\mu, \lambda) = \sum_{n=0}^{\infty} \sum_{p=0}^{\infty} B(n, p) \mu^n \lambda^p \tag{B2}$$

is analytic in the region

$$|\mu| < \frac{1}{4} \quad \text{and} \quad |\lambda| < \frac{1}{2}. \tag{B3}$$

The substitution of (27) and (28) into (B2) gives

$$b(\mu, \lambda) = [\mu f(\mu) - \lambda] / [\mu - \lambda(1-\lambda)], \tag{B4}$$

where

$$f(\mu) = \sum_{n=0}^{\infty} B(n, 0) \mu^n. \tag{B5}$$

The denominator of (B4) vanishes when

$$\lambda = \frac{1}{2} [1 - (1-4\mu)^{1/2}], \tag{B6}$$

which intersects the region (B3). Thus, the numerator

of (B4) must also vanish when (B6) is satisfied. Therefore,

$$f(\mu) = \frac{1}{2} \mu^{-1} [1 - (1-4\mu)^{1/2}], \tag{B7}$$

and, consequently,

$$b(\mu, \lambda) = 2 [1 + (1-4\mu)^{1/2} - 2\lambda]^{-1}. \tag{B8}$$

APPENDIX III

The graph of Fig. 6(a) contains a four-point vertex insertion which is divergent. After renormalization, the contribution from this graph is

$$\begin{aligned}
 \mathfrak{M}' &= iK g^2 G^2 \int_0^\infty \cdots \int_0^\infty dx dx' dudyz \\
 &\quad \times \{ \Delta^{-2} \exp i [xx'(y+z)\Delta^{-1}s + J_1] - (x+x'+u)^{-2} \\
 &\quad \times (y+z)^{-2} \exp i [xx'(x+x'+u)^{-1}s + J_2] \}, \tag{C1}
 \end{aligned}$$

where

$$\Delta = (x+x'+u)(y+z) + yz, \tag{C2}$$

and J_1 and J_2 are independent of s . Again it is sufficient to consider the region of integration where all Feynman parameters are small. For α close to -1 , the Mellin transform of (C1) is approximately

$$\begin{aligned}
 M'(\alpha) &\sim -K g^2 G^2 \int_0^1 \cdots \int_0^1 dx dx' dudyz x^\alpha x'^\alpha \\
 &\quad \times [\Delta^{-2-\alpha} (y+z)^\alpha - (x+x'+u)^{-2-\alpha} (y+z)^{-2}]. \tag{C3}
 \end{aligned}$$

The integration over x can be carried out by (A1) to

give

$$M'(\alpha) \sim -Kg^2G^2(1+\alpha)^{-1} \int_0^1 \cdots \int_0^1 dx' du dy dz \\ \times x'^{\alpha}(y+z)^{-2} \left[\left(x'+u+\frac{yz}{y+z} \right)^{-1} - (x'+u)^{-1} \right]. \quad (C4)$$

The integration over u gives simply

$$M'(\alpha) \sim Kg^2G^2(1+\alpha)^{-1} \int_0^1 \cdots \int_0^1 \frac{dx' dy dz x'^{\alpha}}{(y+z)^2} \\ \times \ln \left[1 + \frac{yz}{x'(y+z)} \right]. \quad (C5)$$

Next the integration over x' yields

$$M'(\alpha) \sim Kg^2G^2(1+\alpha)^{-3} \\ \times \int_0^1 \cdots \int_0^1 dy dz y^{1+\alpha} z^{1+\alpha} (y+z)^{-3-\alpha}. \quad (C6)$$

The right-hand side of (C6) is easily evaluated to give finally

$$M'(\alpha) \sim Kg^2G^2(1+\alpha)^{-4}, \quad (C7)$$

for α near -1 . Hence, as $s \rightarrow \infty$,

$$\mathfrak{M}' \sim \frac{1}{6} Kg^2G^2 s^{-1} (\ln s)^3, \quad (C8)$$

which is negligible when compared with the corresponding quantity for the graph of Fig. 6(b).

Higher Random-Phase Approximations and the Theory of the Electron Gas*

GIU DO DANG AND ABRAHAM KLEIN†

University of Pennsylvania, Philadelphia, Pennsylvania

(Received 12 February 1963)

Using the example of the degenerate electron gas, it is shown how the operator equations of motion for a many-particle system may be exploited to generate systematically a sequence of nonperturbative approximations of which some version of the random-phase approximation is the first. Some questions left unsettled by previous attempts in this direction are resolved by close attention to the structure of the spectrum of the system. The solution of the equations is carried only so far as to make contact with previously substantiated results. Finally, a rigorous proof is given that the plasmon frequency approaches the classical plasmon frequency in the long-wavelength limit.

I. INTRODUCTION

THERE have been several attempts recently to go beyond the extreme high-density limit in the treatment of the problem of the degenerate electron gas in a uniform background of positive charge.¹ Using the diagram techniques developed for the electron gas by Hubbard² and DuBois,³ Osaka⁴ has shown how to sum an infinite but well-defined class of higher order diagrams not previously included in the calculation of the polarization propagator^{2,3} or effective interaction and has applied the results to obtain corrected values of the screening constant, plasmon dispersion relation, and low-temperature specific heat. We shall not be concerned here with this kind of technique, though as we shall show in a sequel to this paper, Osaka's theory coincides with an accurate solution of a suitably defined extended random-phase approximation (RPA).

It is, in fact, well known that the results based on the lowest order polarization propagator are completely equivalent to those which can be obtained from the equation of motion method in the RPA without exchange. It is also well known that the next approximation in the diagram method is equivalent to the *partial inclusion* of the exchange interaction and exchange self-energy effects in the equations of motion i.e., in the use of an extended RPA method as the basis for the theory.⁵ In consequence, several authors have felt that the equation-of-motion method warranted deeper investigation as the foundation for a non-perturbative approach to the many-body problem. Here we mention first the work of Suhl and Werthamer,⁶ whose technique has been applied to nuclear physics by Sawicki.⁷ Their method is based on the extended

* Supported in part by the U. S. Atomic Energy Commission.

† Alfred P. Sloan Foundation Fellow.

¹ For a general discussion, earlier references, and a summary of most of the known results, see D. Pines, *The Many Body Problem* (W. A. Benjamin, Inc., New York, 1961).

² J. Hubbard, Proc. Roy. Soc. (London) **A243**, 336 (1957).

³ D. F. DuBois, Ann. Phys. (N. Y.) **7**, 174 (1959); **8**, 24 (1959).

⁴ Y. Osaka, J. Phys. Soc. Japan **17**, 547 (1962).

⁵ We shall, thus, distinguish between the simple and extended RPA, respectively, where the latter includes exchange and exchange self-energy corrections.

⁶ H. Suhl and N. R. Werthamer, Phys. Rev. **122**, 359 (1961); N. R. Werthamer and H. Suhl, *ibid.* **125**, 1402 (1962). Reference should also be made to the work of K. Sawada, *ibid.* **119**, 2090 (1960).

⁷ J. Sawicki, Phys. Rev. **126**, 2231 (1962); G. Fano and J. Sawicki, Nuovo Cimento **25**, 586 (1962).